

BERICHTE DER BUNSEN-GESELLSCHAFT FÜR PHYSIKALISCHE CHEMIE

AN INTERNATIONAL JOURNAL OF PHYSICAL
CHEMISTRY

Jahresregister von Band 90 (1986)

Herausgeber

Deutsche Bunsen-Gesellschaft für Physikalische Chemie e.V.
Carl-Bosch-Haus, Varrentrappstraße 40/42
D-6000 Frankfurt am Main 90

Telefon (069) 79 17-201

Schriftleiter

Konrad Georg Weil
Institut für Physikalische Chemie
Technische Hochschule Darmstadt
Petersenstraße 20
D-6100 Darmstadt
Telefon (061 51) 16 2498

Alarich Weiss
Institut für Physikalische Chemie
Technische Hochschule Darmstadt
Petersenstraße 20
D-6100 Darmstadt
Telefon (061 51) 16 2607

Redaktion

Redaktion „Berichte der Bunsen-Gesellschaft“
Institut für Physikalische Chemie
Petersenstraße 20, D-6100 Darmstadt

Telefon (061 51) 16 2498

Beratergremium

Ernst Ulrich Franck, Karlsruhe
Friedrich Kohler, Bochum
Werner Kutzelnigg, Bochum
Hermann Schmalzried, Hannover
Heinz Georg Wagner, Göttingen
Gerhard Wegner, Mainz
Albert Weller, Göttingen
Herbert Zimmermann, Freiburg

Verlag



VCH Verlagsgesellschaft mbH
Postfach 1260/1280
D-6940 Weinheim
Federal Republic of Germany
Telefon (06201) 602-0
Telex 465516 vchwh d
Telefax (06201) 602 328

Inhaltsverzeichnis von Band 90 (1986)

(Autorenverzeichnis, Sachverzeichnis, Buchbesprechungen, Personalnachrichten)

A. Autorenverzeichnis

Ache, H. J., siehe Z. B. Alfassi	84	Behner, T., G. Elbers, S. Remme, F. Prissok, P. Stegger, G. Lehmann: Interstitial Transition Metal Impurities as a Possible Cause of Enhanced Reactivities	698	Bordi, F., C. Cametti: Dielectric Properties of Polyelectrolyte Solutions — II. Behaviour of Aqueous Solutions of Carboxymethylcellulose with Divalent Counterions	447
Aguilella, V. M., siehe S. Mafé	476	Behrendt, F., siehe T. Dreier	1010	Borgmann, D., siehe G. Wedler	235
Alavi, M., siehe U. Schneider	746	— siehe B. Roff	1005	Bougeard, D., siehe A. Grunenberg	485
Alfassi, Z. B., H. J. Ache: Temperature Dependence of the Inhibition and Enhancement of Positronium Formation by Pyridine in Decane and Toluene Solutions	84	Bein, Th., M. Tielen, P. A. Jacobs: Zeolite Supported Iron Oxide as Catalyst or Catalyst Precursor for Hydrocarbon Conversion Reactions	395	Bowman, C. T.: Chemical Kinetics Models for Complex Reacting Flows	934
Alter, W., siehe G. Wedler	235	Belkoura, L., siehe D. Schwahn	339	Bredol, M., V. Leute: Thermodynamics and Reactivity in II—VI/III—VI-Systems	714
Anić, S., Lj. Kolar-Anić: Some New Details in the Kinetic Considerations of the Oscillatory Decomposition of Hydrogen Peroxide	539	Benderoth, G., siehe G. H. Kohlmaier	1066	Breen, J., D. van Duijn, J. de Bleijser, J. C. Leyte: Polyethyleneoxide-Dynamics in Aqueous Solutions Studied by Nuclear Magnetic Relaxation	1112
— — The Oscillatory Decomposition of H ₂ O ₂ Monitored by the Potentiometric Method with Pt and Ag ⁺ /S ²⁻ Indicator Electrode	1084	Benje, M., M. Eiermann, U. Pittermann, K. G. Weil: An Improved Quartz Microbalance. Applications to the Electrocrystallization and -dissolution of Nickel	435	Brettel, K., siehe H. T. Witt	1015
Antonucci, V., E. Passalacqua, N. Giordano: Thermally Oxidized Iron Electrodes for Photoelectrochemical Application	828	Bennemann, K. H., siehe H. Dreysse	245	Brickmann, J., siehe P. H. Cribb	162
Asaji, T., siehe S. Fukada	22	Benz, V. W., K. G. Weil: Superstructures on the Polar Faces of Indium Antimonide	201	— siehe P. H. Cribb	168
Asmus, K.-D., siehe J. Mönig	115	Bertagnolli, H., siehe E. Bartsch	34	Brinkmann, U., W. Laqua: Zur Stabilität olivinischer Silikate im Sauerstoffpotentialgradienten. II. Das Kobaltsilikat Co ₂ SiO ₄	680
Backhaus-Ricoult, M.: Diffusion Processes and Interphase Boundary Morphology in Ternary Metal-Ceramic Systems	684	— R. Ehrig, J. U. Weidner, H. W. Zimmermann: Strukturuntersuchung konzentrierter wäßriger Caesiumhydroxid-Lösungen mit Röntgen- und Neutronenstreuung	502	Bröhl, H., siehe G. H. Kohlmaier	1066
— R. Dieckmann: Defects and Cation Diffusion in Magnetite (VII): Diffusion Controlled Formation of Magnetite During Reactions in the Iron-Oxygen System	690	— T. Engelhardt, P. Chieux: Study of Dipolar Interaction in Liquid Pyridine by X-ray and Neutron Diffraction	512	Buss, D. H., siehe J. Bauer	809
Baerns, M., siehe R. Christoph	981	— G. Schulz: An X-ray Study of Specific Bromine Interaction in Liquid Ethylbromine and its Interpretation by Geometrical and Potential Models	816	— siehe J. Bauer	1220
— siehe D. Hess	1234	— siehe H. Weingärtner	1167	Butz, T., A. Lorf: In Situ Studies of Intercalation Reactions Via Nuclear Quadrupole Interactions	638
Ballauff, M.: Calculation of Nematic-Isotropic Phase Equilibria in Solutions of Polymers in Nematic Liquid Crystals Using the Flory Lattice Model	1053	Biasio, A. Di, siehe C. Cametti	621	Cametti, C., siehe F. Bordi	447
Bartsch, E., H. Bertagnolli, P. Chieux: A Neutron and X-Ray Diffraction Study of the Binary Liquid Aromatic System Benzene-Hexafluorobenzene II. The Mixtures	34	Bignell, C. M., siehe P. J. Dunlop	351	— A. Di Biasio: Bulk Counterion Diffusion in Rod-Like Polyelectrolyte Solutions	621
Bauer, E., siehe W. Telieps	197	Binder, K.: Kinetics of the Formation of Ordered Domains on Surfaces: Theoretical Considerations and Monte-Carlo Simulation	257	Cardon, D., siehe D. Vanmaekelbergh	431
— siehe W. Witt	248	— siehe A. Milchev	267	Carlsen, L., siehe H. Egsgaard	369
Bauer, J., D. H. Buss, O. Glemser: The Electrochemical Behaviour of Manganese(II)-Hydroxide/Magnesium Hydroxide and Manganese(II)-Hydroxide/Calcium Hydroxide	809	Bleijser, J. de, siehe J. Breen	1112	Carter, C. B.: Interfaces in Solid-State Reactions	643
— D. H. Buss, O. Glemser: Preparation and Electrochemical Behaviour of Doped Manganese Dioxide	1220	Blümich, B., siehe S. Jurga	1153	— Y. Kouh Simpson: Thin-Film Reactions	676
Becker, F., siehe U. Kramer	521	Blumen, A., G. Zumofen, J. Klafter: Reactions in Disordered Media, Modelled Through Hierarchical Structures	1048	Castro, A., E. Iglesias, J. R. Leis, M. E. Peña: A Kinetic Study of the Diazotization of Substituted 1-Naphthylamines	891
Becker, R., H. Lentz, E. Hinze, G. Nover, G. Will: Ein Quecksilberporosimeter hoher Präzision zur Charakterisierung mineralischer Stoffe	833	Böhland, T., F. Temps, H. Gg. Wagner: A Direct Study of the Reaction CH ₂ (\bar{X}^3B_1) + C ₂ H ₄ in the Temperature Range 296 K ≤ T ≤ 728 K	468	Cemic, L., St. Grammenopoulou-Bilal, K. Langer: A Microscope-Spectrometric Method for Determining Small Fe ³⁺ -Concentrations Due to Fe ³⁺ -Bearing Defects in Fayalite	654
Beckmann, W., R. Lacmann: On Some Aspects of the Modelling of the Crystal Growth	963	Böhm, M. C., P. C. Schmidt: Electronegativities and Hardnesses of the Main Group Elements from Density Functional Theory: Dependence on the Hybridization of the Chemical Bond	913	Chieux, P., siehe E. Bartsch	34
Behm, R. J., siehe W. Höslner	205	Borchers, D., A. Weiss: Structure, Hydrogen Bonds and Phase Transition in Ethylenediammonium Hexachlorometallates, [H ₃ N(CH ₂) ₂ NH ₃] ^{2⊕} [XCl ₆] ^{2⊖} , X = Sn, Pb, Te, Pt. A ³⁵ Cl NQR and X-ray Diffraction Study	718	— siehe H. Bertagnolli	512
— G. Ertl, J. Wintterlin: On the Kinetics and Mechanisms of the Oxygen Induced (2 × 1) Reconstruction of Ni(110)	294			Christmann, K.: Phase Transitions in Chemisorbed Hydrogen Layers	307

I. One Dimensional Model Approach	162	thane Radical Cation in the Gas Phase	369	Fojtik, A., siehe Ch.-H. Fischer	46
— Time Delayed Two Photon Processes: II. Duschinsky Mixing Effects	168	Fhrig, R., siehe H. Bertagnolli	502	Frahm, J., siehe K.-D. Merboldt	614
Damjanovic, A., D. B. Sepa, Lj. M. Vracar, M. V. Vojnovic: A Comment on the β -Factor and Enthalpy of Activation for Oxygen Reduction at Pt and Au Electrodes	1231	Eicke, H.-F., S. Geiger, F. A. Sauer, H. Thomas: Dielectric Study of Fractal Clusters Formed by Aqueous Nanodroplets in Apolar Media	872	Franck, E. U., siehe M. Gehrig	525
Dékány, I., F. Szántó, Ar. Weiss, G. Lagaly: Interactions of Hydrophobic Layer Silicates with Alcohol-Benzene-Mixtures; I. Excess and Model Adsorption Isotherms	422	Eiermann, M., siehe M. Benje	435	— siehe M. Christoforakos	780
— Interactions of Hydrophobic Layer Silicates with Alcohol-Benzene Mixtures; II. Structure and Composition of the Adsorption Layer	427	Elbel, S., siehe H. Egsgaard	369	Freund, A., Th. Kruel, F. W. Schneider: Distinction Between Deterministic Chaos and Amplification of Statistical Noise in an Experimental System	1079
Deuffhard, P., U. Nowak: Efficient Numerical Simulation and Identification of Large Chemical Reaction Systems	940	Elbers, G., siehe T. Behner	698	Freund, H.-J., siehe D. Schmeißer	228
Dickens, P. G., siehe S. J. Hibble	702	Eldik, R. van, siehe P. Martinez	609	Fromme, P., siehe P. Gräber	1034
Dieckmann, R., H. Schmalzried: Defects and Cation Diffusion in Magnetite (VI): Point Defect Relaxation and Correlation in Cation Tracer Diffusion	564	Elias, E., N. Hoang, J. Sommer, B. Schramm: Die zweiten Virialkoeffizienten von Helium-Gasmischungen im Bereich unterhalb Zimmertemperatur	342	Fuess, H., E. Stuckenschmidt, B. P. Schweiss: Inelastic Neutron Scattering Studies of Water in Natural Zeolites	417
— siehe M. Backhaus-Ricoult	690	Embid, J. M., siehe S. Otin	1179	— L. Schröpfer, H. Feuer: Exsolution and Phase Transformations in Synthetic Pyroxenes. X-ray and TEM-Studies at Elevated Temperatures	755
Ditzel, A., F. Wasgestian: Deuterium Isotope Effect in the Photophysics of Chromium (III) Alkylamine Complexes	111	Emig, G.: Reaktormodelle für heterogen katalysierte Gasphasenreaktionen	968	Fujara, F., siehe S. Jurga	1153
Dohrmann, J. K., U. Sander: In Situ Photoacoustic Spectroscopy of Electrochemically Grown PbO ₂ Films. Optical Constants from Photoacoustic Interference Signals	605	Endo, H., siehe H.-P. Seyer	587	Fujisaki, M., T. Gäumann, A. Ruf: Kinetic Isotope Effects for Hydrogen Abstraction from Various Saturated Hydrocarbons by Deuterium Atoms in the Gas Phase	375
Dowben, P. A., siehe D. Mueller	281	Engelhardt, T., siehe H. Bertagnolli	512	Fukada, S., K. Horiuchi, T. Asaji, D. Nakamura: Structural Phase Transition in Orthorhombic and Monoclinic Fe ³⁺ Doped K ₃ Co(CN) ₆ Crystals as Studied by the Temperature Variation of ¹⁴ N NQR Frequencies	22
Dreeskamp, H., A. G. E. Läufer: Solvent Influence on (Perylene ... Ag ⁺)* Exciplex Fluorescence	1195	Ertl, G.: Reactive Transformation of Surface Structure	284	— siehe R. J. Behm	294
Dreier, T., B. Lange, J. Wolfrum, M. Zahn, F. Behrendt, J. Warnatz: Comparison of CARS Measurements and Calculations of the Structure of Laminar Methane-Air Counterflow Diffusion Flames	1010	Fabian, P., siehe B. C. Krüger	1062	Funk, K.: Debye-Hückel-Type Relaxation Processes in Solid Electrolytes: Complex Conductivity Arcs and Broad Quasielastic Neutron Scattering	661
Dreysé, H., D. Tománek, K. H. Bennemann: Calculation of Interactions Between Adsorbates on Transition Metal Surfaces	245	Fahr, A., siehe D. A. Robaugh	77	Gadooni, J., U. Onken: Catalysis of Hydrazine Oxidation by Sulphonated Phthalocyanines	154
Driessens, F. C. M.: Thermodynamics of Ionic Solid Solutions and Its Application to the Formation and Stability of Biominerals	760	Fain, S. C. Jr.: Structures and Phase Transitions in Physisorption: Molecular-Axis Orientational Ordering in Nitrogen and Carbon Monoxide Monolayers on Graphite	211	Gärtner, G., P. Janiel, H. Rau, H. A. M. van Hal, H. J. P. Nabben: Flow Method Vapour Pressure Determination and Characterization of Tetrakis-(Trifluoropentanedionato)-Thorium(IV) and Tetrakis (Heptafluorodimethyloctanedionato)-Thorium(IV)	459
Duijn, D. van, siehe J. Breen	1112	Fecher, G., Al. Weiss: On the Order-Disorder Phase Transition of Anilinium Halides. Crystal Structure of the High and Low Temperature Phase of Anilinium Iodide, C ₆ H ₅ NH ₃ ⁺ I ⁻ (C ₆ D ₅ NH ₃ ⁺ I ⁻). X-ray and Neutron Diffraction Studies	1	M. van Hal, H. J. P. Nabben: Flow Method Vapour Pressure Determination and Characterization of Tetrakis-(Trifluoropentanedionato)-Thorium(IV) and Tetrakis (Heptafluorodimethyloctanedionato)-Thorium(IV)	459
Dunlop, P. J., C. M. Bignell, H. L. Robjohns: Excess and Interaction Second Virial Coefficients for Twelve Binary Gaseous Systems Containing Carbon Tetrafluoride	351	Fecher, G., Al. Weiss: On the Order-Disorder Phase Transition of Anilinium Halides. ¹²⁷ I-NQR Investigation of the Anilinium Iodides C ₆ H ₅ NH ₃ ⁺ I ⁻ , C ₆ H ₅ ND ₃ ⁺ I ⁻ , C ₆ D ₅ NH ₃ ⁺ I ⁻ , and C ₆ D ₅ ND ₃ ⁺ I ⁻ . Dilatometric Studies on Anilinium Bromide and Anilinium Iodide Single Crystals	10	Gäumann, T., siehe M. Fujisaki	375
Duschner, H., siehe U. Schneider	746	Felsche, J., S. Luger: Structural Collapse or Expansion of the Hydro-Sodalite Series Na ₈ [AlSiO ₄] ₆ (OH) ₂ · nH ₂ O and Na ₆ [AlSiO ₄] ₆ · nH ₂ O Upon Dehydration	731	Gardiner, W.: Parameter Optimization in Detailed Chemical Kinetics Modeling	1024
Ebert, K. H., siehe U. Stabel	1001	Fernández, J., siehe S. Otin	1179	Gehrig, M., H. Lentz, E. U. Franck: The System Water — Carbon Dioxide — Sodium Chloride to 773 K and 300 MPa	525
Eder, S., K. Markert, A. Jablonski, K. Wandelt: Substrate Dependence of the 2D Gas-Solid Phase Transition in Adsorbed Xenon Layers	225	Feuer, H., siehe H. Fuess	755	Geiger, S., siehe H.-F. Eicke	872
Ederer, H. J., siehe U. Stabel	1001	Fischer, Ch.-H., H. Weller, A. Fojtik, C. Lume-Pereira, E. Janata, A. Henglein: Photochemistry of Colloidal Semiconductors 10. Exclusion Chromatography and Stop Flow Experiments on the Formation of Extremely Small CdS Particles	46	Gerhardt, M., H. Schuster, P. J. Plath: Ein diskretes mathematisches Modell für die Dynamik der Methanoloxidation an einem Palladium-Trägerkatalysator	1040
Edwards, P. P., siehe D. E. Logan	575	Fischer, J., Al. Weiss: Transport Properties of Liquids. IV. Self-Diffusion, Viscosity, and Mass Density of Ellipsoidal Shaped Molecules in the Pure Liquid Phase	896	Giordano, N., siehe V. Antonucci	828
Egsgaard, H., L. Carlsen, S. Elbel: Isomerizations of the Nitrome-		— Transport Properties of Liquids VI. Viscosity, Excess Volumes, and Self-Diffusion of Nearly Athermal Mixtures	1129	Glemser, O., siehe J. Bauer	809
		— Transport Properties of Liquids VII. Viscosity, Excess Volumes, and Self-Diffusion of Binary Mixtures of Donor-Acceptor and of CCl ₄ -Carboxylic Acid Systems	1141	— siehe J. Bauer	1220
				Gomes, W. P., siehe D. Vanmaekelbergh	431
				Goslich, R., siehe J. Mönig	115
				Gräber, P., P. Fromme, U. Junesch, G. Schmidt, G. Thulke: Kinetics of Proton-Transport-Coupled ATP Synthesis Catalyzed by the Chloroplast ATP Synthase	1034
				Grammenpopoulou-Bilal, St., siehe L. Cemic	654
				Gray, P., S. K. Scott: A New Model for Oscillatory Behaviour in Closed Systems: The Autocatalator	985
				Greuter, F., siehe D. Schmeißer	228

- Grunenberg, A., D. Bougeard: The Observed and Calculated Vibrational Spectra of DL-methionine in the Study of the Solid State Phase Transition 485
- Güsten, H., siehe M. Rinke 439
- Gunßer, W., siehe G. J. Harms 764
- Hack, W., H. Kurzke, P. Rouvelles, H. Gg. Wagner: Hydrogen Abstraction Reactions by $\text{NH}_2(\bar{X}^2\text{B}_1)$ -Radicals from Hydrocarbons in the Gas Phase 1210
- Häfele, E., H.-G. Lintz: Oxide Formation during the Reaction of Carbon Monoxide and Oxygen on Polycrystalline Platinum 298
- Hal, van H. A. M., siehe G. Gärtner 459
- Handwerk, V., R. Zellner: Kinetics and Energetics of the Reaction $\text{ClO} + \text{O}_2(^1\Delta_2) \rightarrow \text{ClO}_3$ 92
- Harbison, G. S., siehe S. Jurga 1153
- Harms, G. J., W. Gunßer: Wet Salt Melts – A Reaction Medium Suitable for the Preparation of Metastable Oxides and Hydroxides? 764
- Hauck, J.: Interstitial Site Occupancy of Hydrogen Atoms in Laves Phases and Structurally Related Compounds 708
- Hcakal, F. El-Taib, siehe A. A. Mazhar 1205
- Heckl, W. M., H. Möhwald: A Narrow Window for the Observation of Spiral Lipid Crystals 1159
- Heier, H. J., siehe H. Pfnür 272
- Heintz, A., siehe H. Wagner 463
- Heinze, J., M. Störzbach: Electrochemistry at Ultramicroelectrodes – Simulation of Heterogeneous and Homogeneous Kinetics by an Improved ADI-technique 1043
- Henglein, A., siehe Ch.-H. Fischer 46
- Henkel, T., siehe N. Vennemann 888
- Hensel, F., siehe K. Tamura 581
- siehe H.-P. Seyer 587
- Hermanns, H. D., siehe K. Nataraajan 533
- Hess, D., H. Papp, M. Baerns: Fe/Mn Oxide Catalysts for the Fischer-Tropsch-Synthesis; Part VII: Adsorption of Carbon Monoxide and Nitrogen at Low Temperatures 1234
- Heydtmann, H., siehe F. G. Simon 543
- Hibble, S. J., P. G. Dickens: Structure and Thermodynamics of H-Insertion in Mo(W) -Oxides 702
- Hinze, E., siehe R. Becker 833
- Hiraiwa, J., siehe W. Ueda 353
- Hoang, N., siehe E. Elias 342
- Hösler, W., E. Ritter, R. J. Behm: Topological Aspects of the $(1 \times 1) \rightleftharpoons$ "Hexagonal" Phase Transition on $\text{Pt}(100)$ 205
- Hoffmann, H., G. Platz, W. Ulbricht: From Micellar Solutions to Microemulsions – A Kinetic Study – siehe H. Rehage 877
- Hofmann, W. K., R. Könenkamp, Th. Schwarzlose, M. Kunst, H. Tributsch, H. J. Lewerenz: Melt Grown Layered Crystals: Comparison of Optoelectronic Properties 824
- Hoja, R., siehe R. Marx 222
- Homann, K. H., U. v. Pidoll: The Low-Pressure Pyrolysis of Butadiene (C_4H_2) 847
- Horiuchi, K., siehe S. Fukada 22
- Hoshino, H., siehe H.-P. Seyer 581
- Husain, D., G. Roberts: Kinetic Investigation of (a) the Collisional Quenching of $\text{Mg}(3^3\text{P}_1)$ by CO_2 over the Temperature Range 600–1100 K by Time-Resolved Atomic Emission ($\text{Mg}(3^3\text{P}_1) \rightarrow \text{Mg}(3^1\text{S}_0) + h\nu$) and (b), $E - (E, V)$ Transfer from $\text{Mg}(3^3\text{P}_1)$ to MgO by Time-Resolved Molecular Emission ($\text{MgO}, \text{B}^1\Sigma^+ - \text{A}^1\Pi$ and $\text{B}^1\Sigma^+ - \text{X}^1\Sigma^+$) Following Pulsed Dye-Laser Excitation at $\lambda = 457.1 \text{ nm}$ ($\text{Mg}(3^3\text{P}_1) \leftarrow \text{Mg}(3^1\text{S}_0)$) 360
- Hussla, I., H. Coufal, F. Träger, T. J. Chuang: Pulsed Laser-Induced Thermal Desorption of Xenon 240
- Iglesias, E., siehe A. Castro 891
- Ikeda, R., siehe A. Kubo 479
- siehe H. Ishida 598
- Ise, N., siehe Y. Ishii 50
- Ishida, H., R. Ikeda, D. Nakamura: Cationic Motions Involving Self-Diffusion and Structural Phase Transitions in Solid Dimethyl- and Trimethylammonium Nitrates as Studied by Differential Thermal Analysis and ^1H NMR Techniques 598
- Ishizuka, Y., siehe Y. Nosaka 1199
- Ishii, Y., H. Matsuoka, N. Ise: "Ordered" Distribution of Ionic Micelles in Dilute Solutions of Alkyltrimethylammonium Chloride as Studied by Small-Angle X-ray Scattering 50
- Ishikawa, H., siehe O. Uemura 71
- Itami, T., siehe Y. Morikawa 1174
- Jablonski, A., siehe S. Eder 225
- Jacobs, P. A., siehe Th. Bein 395
- Jaeger, N. I., R. Ottensmeyer, P. J. Plath: Oscillations and Coupling Phenomena Between Different Areas of the Catalyst During the Heterogeneous Catalytic Oxidation of Ethanol 1075
- Janata, E., siehe Ch.-H. Fischer 46
- Janecek, A., siehe G. H. Kohlmaier 1066
- Janiel, P., siehe G. Gärtner 459
- Joshi, Y. P., D. J. Tildesley: Scaled-Particle Theory for Adsorbed Hard-Core Molecules 217
- Junesch, U., siehe P. Gräber 1034
- Jurga, S., G. S. Harbison, B. Blümich, H. W. Spiess, F. Fujara, A. Olinger: Static and MAS ^{35}Cl NMR and Molecular Motions of ClO_4^- Ions in the Various Phases of Multimethylammonium Perchlorates 1153
- Kabadi, V. N.: Molecular Dynamics of Fluids: The Gaussian Overlap Model II 327
- Statistical Mechanics of Non-Spherical Molecules: Spherical Harmonic Expansions on Non-Spherical Surfaces. II. Gay-Berne Gaussian Overlap Potential 332
- Kalidas, C., siehe A. Palanivel 794
- Karhäuser, J., siehe I. Wagner 861
- Kassmann, K.-D., H. Knapp: Vapor-Liquid Equilibria for Binary and Ternary Mixtures of Benzene, Toluene and n-Butyraldehyde 452
- Kerl, K.: Reduced Representation of Second Virial Coefficients by Straight Lines 789
- Kind, M., siehe A. Mersmann 955
- Kishimoto, S., siehe W. Ueda 353
- Klafter, J., siehe A. Blumen 1048
- Kleinfeld, M., H.-D. Wiemhöfer: Chemical Diffusion in CuInS_2 in the Temperature Range of 20°C to 100°C 711
- Klump, H.: Experimental Evaluation of the B-DNA \rightarrow Z-DNA Transition: Energetics of a Reversible, Thermally Induced Helix/Helix Transition of Poly dG-m ^2C in Physiological Mg^{2+} Concentrations 444
- Knapp, H., siehe K.-D. Kassmann 452
- Knoll, W., siehe N. Vennemann 888
- Koçak, M., siehe U. Kramer 521
- Könenkamp, R., siehe W. K. Hofmann 824
- Kohlmaier, G. H., H. Bröhl, A. Janecek, G. Benderoth: Modellierung des Kohlenstoffaustauschs zwischen Atmosphäre und Landvegetation unter Berücksichtigung von Landnutzungsänderungen und CO_2 -Düngungseffekt 1066
- Kolar-Anić, Lj., siehe S. Anić 539
- siehe S. Anić 1084
- Koster, T. P. M., siehe A. H. A. Tinnemans 383
- siehe A. H. A. Tinnemans 390
- Kouh Simpson, Y., siehe C. B. Carter 676
- Kramer, U., M. Koçak, A. Steiger, F. Becker: Excess Enthalpies of Binary Liquid Mixtures Containing Oxiranes. Part 1: H^E (298.15 K, 101.3 kPa) of the Four Systems Chloromethyl- and Bromomethyl-Oxirane + n-Hexane and n-Heptane 521
- Krüger, B. C., P. Fabian: Model Calculations About the Reduction of Atmospheric Ozone by Different Halogenated Hydrocarbons 1062
- Kruel, Th., siehe A. Freund 1079
- Kubo, A., R. Ikeda, D. Nakamura: Self-Diffusion, Overall Rotation of Molecules, and Ring Motions in the Three Solid Phases of Formylferrocene, $\text{Fe}(\text{C}_5\text{H}_5)(\text{C}_5\text{H}_4\text{CHO})$, as Studied by ^1H NMR and Differential Thermal Analysis 479
- Kuhn, H., siehe Y. Yonezawa 1183
- Kunst, M., siehe W. K. Hofmann 824
- Kurzke, H., siehe W. Hack 1210
- Lacmann, R., siehe W. Beckmann 963
- Läufer, A. G. E., siehe H. Dreeskamp 1195
- Lagally, M. G., siehe M. Tringides 277
- Lagaly, G., siehe I. Dékány 422
- siehe I. Dékány 427
- Lange, B., siehe T. Dreier 1010
- Langer, K., siehe L. Cemic 654
- Laqua, W., siehe U. Brinkmann 680
- Leaist, D. G.: Mass Transport in Aqueous Zinc Chloride-Potassium Chloride Electrolytes 797
- Lechner, M. D., siehe N. Vennemann 888
- Lehmann, G., siehe T. Behner 698
- Leis, J. R., siehe A. Castro 891
- Lengeler, B.: Internal Oxidation of Impurities in Palladium Investigated by X-ray Absorption Spectroscopy 649
- Lentz, H., siehe M. Gehrig 525
- siehe R. Becker 833
- Lerf, A., siehe T. Butz 638
- Leute, V., siehe M. Bredol 714
- Lewerenz, H. J., siehe W. K. Hofmann 824
- Leyte, J. C., siehe J. Breen 1112

- Lichtenthaler, R. N., siehe H. Wagner 65
 — siehe H. Wagner 69
 — siehe H. Wagner 463
 Limbach, H.-H., siehe G. Otting 1122
 Lintz, H.-G., siehe E. Häfele 298
 Logan, D. E., P. P. Edwards: Frenkel Excitonic Insulator Transitions in Expanded Metals 575
 Losa, C. G., siehe S. Otin 1179
 Luger, S., siehe J. Felsche 731
 Lume-Pereira, C., siehe Ch.-H. Fischer 46
 Lyo, I. W., siehe D. Schmeißer 228
- Mackor, A., siehe A. H. A. Tinnemans 383
 — siehe A. H. A. Tinnemans 390
 Mafé, S., J. Pellicer, V. M. Aguilera: The Goldman Constant Field Assumption: Significance and Applicability Conditions 476
 Maier, J.: On the Conductivity of Polycrystalline Materials 26
 — B. Reichert: Ionic Transport in Heterogeneously and Homogeneously Doped Thallium(I)-Chloride 666
 Maier, E., G. Olbrich: The Synchronous 1,4-Addition of $\text{SiH}_2(\text{A}_1)$ to *s-cis*-buta-1,3-diene. A CI and CASSCF Study 86
 Malic, R. A., siehe E. G. McRae 268
 Markert, K., siehe S. Eder 225
 Martinez, P., R. Mohr, R. van Eldik: The Effect of Ionic Strength and Pressure on the Complex Formation Kinetics of the Aquated Iron(II)-Thiocyanate System 609
 Marx, R., R. Hoja: 2d Krypton, a Model System for a Commensurate-Incommensurate Transition 222
 Matsuoka, H., siehe Y. Ishii 50
 Mazhar, A. A., F. El-Taib Heakal: Retardation of the Cd^{2+} and In^{3+} Reduction Processes at DME in Chloride Medium in Relation to Adsorption of Coumarin 1205
 McRae, E. G., R. A. Malic: A $7 \times 7 \rightarrow 2 \times 7$ Phase Transition of Au Overlayers on Ni(110) Surface 268
 Merboldt, K.-D., J. Frahm: ^1H -NMR Relaxation Study of Water in Binary Solvent Mixtures in the Absence and Presence of Electrolytes 614
 Mersmann, A., M. Kind: Modellierung in der Verfahrenstechnik am Beispiel von Kristallisatoren 955
 Meschede, L., siehe G. Otting 1122
 Milchev, A., K. Binder: Monte Carlo Study of a Lattice Gas Model with Nonadditive Lateral Interactions 267
 Miyama, H., siehe Y. Nosaka 1199
 Möbius, D., siehe Y. Yonezawa 1183
 Möhwald, H., siehe W. M. Heckl 1159
 Möller, W., E. Mozzhukhin, H. Gg. Wagner: High Temperature Reactions of CH_3 ; 1. The Reaction $\text{CH}_3 + \text{H}_2 \rightarrow \text{CH}_4 + \text{H}$ 854
 Mönig, J., R. Goslich, K.-D. Asmus: Thermodynamics of $\text{S} \cdot \text{S} \ 2\sigma/1\sigma^*$ Three-electron Bonds and Deprotonation Kinetics of Thioether Radical Cations in Aqueous Solution 115
 Mohr, R., siehe P. Martinez 609
 Morikawa, Y., T. Itami, M. Shimoi: The Volume of Liquid Hg-In and Hg-Sn Alloys 1174
 Moritz, W., siehe M. Tringides 277
- Mostafa, S. N., S. R. Selim: Electrochemical and Thermodynamic Studies on Copper-Silver-Selenium System 130
 Mozzhukhin, E., siehe W. Möller 854
 Mueller, D., T. N. Rhodin, P. A. Dowben: Halogen Overlayer Structures on Fe(110) 281
 Müller, K.: Relaxation and Reconstruction of Solid Surfaces 184
 Müller-Warmuth, W., siehe E. Wein 158
 — siehe Cl. Ritter 357
 Müser, H. E., siehe F. S. Rys 291
- Nabben, H. J. P., siehe G. Gärtner 459
 Nakahara, M., siehe Y. Yoshimura 58
 Nakamura, D., siehe S. Fukada 22
 — siehe A. Kubo 479
 — siehe H. Ishida 598
 Nakamura, K., T. Østvold, H. A. Øye: Vapour Pressure of Molten Acidic Potassium Chloride-Aluminium Chloride-Aluminium Chloride Monoamine Mixtures 141
 Natarajan, K., K. Thielen, H. D. Hermanns, P. Roth: Thermal Decomposition of Cyanogen Measured in $\text{C}_2\text{N}_2/\text{O}_2$ and $\text{C}_2\text{N}_2/\text{H}_2$ Reaction Systems by Atomic Resonance Absorption 533
 Nosaka, Y., Y. Ishizuka, H. Miyama: Separation Mechanism of a Photoinduced Electron-Hole Pair in Metal-loaded Semiconductor Powders 1199
 Nover, G., siehe R. Becker 833
 Nowak, U., siehe P. Deuffhard 940
- Olbrich, G., siehe E. Maier 86
 Olinger, A., siehe S. Jurga 1153
 Onken, H. U., E. Wicke: Statistical Fluctuations of Temperature and Conversion at the Catalytic CO Oxidation in an Adiabatic Packed Bed Reactor 976
 Onken, U., siehe J. Gadooni 154
 Østvold, T., siehe K. Nakamura 141
 Oswald, H. R., A. Reller: Einflüsse struktureller Gegebenheiten auf den Verlauf von heterogenen Festkörperreaktionen 671
 Otin, S., J. Fernández, J. M. Embid, I. Velasco, C. G. Losa: Thermodynamic and Dielectric Properties of Binary Polar + Non-Polar Mixtures; I. Static Dielectric Constants and Excess Molar Enthalpies of *n*-Alkylamine + *n*-Dodecane Systems 1179
 Otting, G., H. Rumpel, L. Meschede, G. Scherer, H.-H. Limbach: Dynamic Liquid State NMR and IR Study of Tautomerism and Conformations of Tetraphenylloxalamidine, a Novel Small Intramolecular Double Hydrogen Transfer System 1122
 Øye, H. A., siehe K. Nakamura 141
 Ottensmeyer, R., siehe N. I. Jaeger 1075
- Palanivel, G. Rajendran, C. Kalidas: Selective Solvation of Some Silver(I) Salts in Water-Pyridine Mixtures at 30°C 794
 Pannetier, J.: Real-Time Neutron Powder Diffraction: A Technique for the Study of Solid State Reactions 634
 Papp, H., siehe D. Hess 1234
 Passalacqua, E., siehe V. Antonucci 828
 Pellicer, J., siehe S. Mafé 476
 — S. Mafé, V. M. Aguilera: Ionic Transport Across Porous Charged Membranes and the Goldman Constant Field Assumption 867
 Peña, M. E., siehe A. Castro 891
 Pfnür, H., H. J. Heier: Order-Disorder Phenomena in the System CO/Ru(001) 272
 Piazza, S., siehe F. Di Quarto 549
 Pidoll, U. v., siehe K. H. Homann 847
 Pittermann, U., siehe M. Benje 435
 Plath, P. J., siehe M. Gerhardt 1040
 — siehe N. I. Jaeger 1075
 Platz, G., siehe H. Hoffmann 877
 Plummer, E. W., siehe D. Schmeißer 228
 Prestel, H., U. Schindewolf: Thermodynamics, Conductivity and Photochemical Effects of Sulphur Ammonia Solutions 150
 Prinz, D., L. Riekert: Observation of Rates of Sorption and Diffusion in Zeolite Crystals at Constant Temperature and Pressure 413
 Prissok, F., siehe T. Behner 698
- Quarto, F. Di, C. Sunseri, S. Piazza: Amorphous Semiconductor-Electrolyte Junction. A New Interpretation of the Impedance Data of Amorphous Semiconducting Films on Metals 549
- Raffel, B., J. Wolfrum: Infrared Laser Induced Ignition of Gas Mixtures 997
 Raineri, F. O., E. O. Timmermann: Influence of Ionic Traces Upon the Electric Conductivity of an Electrolyte Solution. On the Possibility of Obtaining the Trace Mobility of an Ion Exclusively by Conductance Measurements 802
 Rajendran, G., siehe A. Palanivel 794
 Rau, H., siehe G. Gärtner 459
 Ray, W. H.: Modelling of Polymerization Phenomena 947
 Rehage, H., H. Hoffmann, I. Wunderlich: A Rheological Switch: Shear Induced Phase Transitions in Aqueous Surfactant Solutions 1071
 Reichert, B., siehe J. Maier 666
 Reller, A., siehe H. R. Oswald 671
 — Reversible Reduktions- und Reoxidationsprozesse des Typs $\text{ABO}_3 \rightleftharpoons \text{ABO}_{3-x}$ an Perovskitischen Metalloxiden 742
 — siehe H. R. Oswald 671
 Remme, S., siehe T. Behner 698
 Rhodin, T. N., siehe D. Mueller 281
 Ricoult, D. L., H. Schmalzried: Periodic Precipitation During Internal Oxidation of Iron-Doped Magnesium Oxide Crystals 135
 Riekert, L., siehe D. Prinz 413
 Rinke, M., H. Güsten: Optische Aufheller als Laserfarbstoffe 439
 Ritter, Cl., W. Müller-Warmuth, R. Schöllhorn: A Further ^1H NMR Study on Cubic H_xWO_3 : Reasons for the Apparent "Prefactor Anomaly" 357
 Ritter, E., siehe W. Hösler 205
 Robaugh, D. A., W. Tsang, A. Fahr, S. E. Stein: Ethylbenzene Pyrolysis: Benzyl C—C or C—H Bond Homolysis 77
 Roberts, G., siehe D. Husain 360
 Robjohns, H. L., siehe P. J. Dunlop 351
 Rogg, B., F. Behrendt, J. Warnatz: Modelling of Turbulent Methane-Air Diffusion Flames: The Laminar-Flamelet Model 1005

- Roth, P., siehe K. Natarajan 533
Rouveilletes, P., siehe W. Hack 1210
Rüsenberg, M., H. Viehhaus: Reversible and Irreversible Phase Transitions in the Surface Segregation of Sn, Sb, and Al on Iron Single Crystals 301
Ruf, A., siehe M. Fujisaki 375
Rumpel, H., siehe G. Otting 1122
Rys, F. S.: Roughening of Solid Surfaces 208
– H. E. Müser: Statistical Model for the Hydrogen-Induced Reconstruction of the Ni(110) Surface 291
Sander, U., siehe H. Ishida 598
Satow, T., siehe O. Uemura 71
Sauer, F. A., siehe H.-F. Eicke 872
Saygin, Ö., siehe H. T. Witt 1015
Scherer, G., siehe G. Otting 1122
Schindewolf, U., siehe H. Prestel 150
Schlodder, E., siehe H. T. Witt 1015
Schmalzried, H., siehe D. L. Ricoult – siehe R. Dieckmann 564
Schmeißer, D., I. W. Lyo, F. Greuter, E. W. Plummer, H.-J. Freund, M. Seel: Photoemission from Ordered Physisorbed Molecular Phases N₂/Graphite, N₂ and CO/Ag(111) 228
Schmidt, G., siehe P. Gräber 1034
Schmidt, P. C., siehe M. C. Böhm 913
Schmidt, R.: The Endoperoxide of Mesodiphenylhelianthrene. Four Reaction Channels Leading from Different Upper Excited Electronic States to Cycloreversion 813
Schmidtke, H.-H., siehe A. Urushiyama 1188
Schneider, F. W., siehe A. Freund 1079
Schneider, M., J. Wolfrum: Mechanisms of By-Product Formation in the Dehydrochlorination of 1,2-Dichloroethane 1058
Schneider, U., M. Alavi, H. Duschner: An Experiment for Determining the Kinetics of Heterogeneously Catalyzed Gas Reactions 746
Schöllhorn, R., siehe E. Wein 158
– siehe Cl. Ritter 357
Schönherr, Th., siehe A. Urushiyama 1188
Schoonman, J., siehe A. H. A. Tinnemans 383
– siehe A. H. A. Tinnemans 390
Schramm, B., siehe E. Elias 342
Schreyer, W.: The Mineral Cordierite: Structure and Reactions in the Presence of Fluid Phases 748
Schröpfer, L., siehe H. Fuess 755
Schulz, G., siehe H. Bertagnoli 816
Schumacher, R., siehe D. M. Teschner 593
Schuster, H., siehe M. Gerhardt 1040
Schwahn, D., L. Belkoura, D. Woermann: Neutron Scattering Experiments with a Binary Critical Mixture for the Determination of the Critical Exponent η 339
Schwahn, P., D. Woermann: Transport of Ions Against their Concentration Gradient Across Cation Exchange Membranes 773
Schwarzlose, Th., siehe W. K. Hofmann 824
Schweiss, B. P., siehe H. Fuess 417
Scott, S. K., siehe P. Gray 985
Seel, M., siehe D. Schmeißer 228
Sekiya, T., siehe O. Uemura 71
Selim, S. R., siehe S. N. Mostafa 130
Selke, W.: Wetting Phenomena at Domain Boundaries 232
Sepa, D. B., siehe A. Damjanovic 1231
Seyer, H. P., siehe K. Tamura 581
– K. Tamura, H. Hoshino, H. Endo, F. Hensel: The Optical Properties of Liquid Se and Se_{1-x}Tc_x Alloys 587
Sharma, S., N. Weiden, A. Weiss: Order-Disorder in Solid 1,2,3-Trichlorobenzene. A Single Crystal ³⁵Cl NQR Study 725
Shimoi, M., siehe Y. Morikawa 1174
Shimokawa, S.: Nuclear Spin-lattice Relaxation and Self-diffusion Coefficient for Toluene around Supercritical Region 126
Simon, F. G., H. Heydtmann: Bestimmung der Geschwindigkeitskonstanten der Reaktion von ¹CH₂ mit Fluor- und Chlorethen 543
Siré, E.-O.: On Topological-Dynamical Equivalent Representations of Reaction Networks: The Omega-Equation and a Canonical Class of Mass Action Kinetics 1087
Solomon, T.: Coverage Dependence of CO Electrosorption on Palladium: An *in-situ* IR Study 556
Sommer, J., siehe E. Elias 342
Spiess, H. W., siehe S. Jurga 1153
Stabel, U., H. J. Ederer, K. H. Ebert: The Modelling of Gasphase Aromatisation in the Pyrolysis of Hydrocarbons (Part II) 1001
Stegger, P., siehe T. Behner 698
Steiger, A., siehe U. Kramer 521
Stein, S. E., siehe D. A. Robaugh 77
Stephan, W.: Nonlinear Phenomena in the Evolution of Satellite DNA 1029
Strehlow, H., siehe I. Wagner 861
Stritzker, B., siehe D. M. Teschner 593
Störzbach, M., siehe J. Heinze 1043
Stuckenschmidt, E., siehe H. Fuess 417
Sunseri, C., siehe F. Di Quarto 549
Szántó, F., siehe I. Dékány 422
– siehe I. Dékány 427
Tamura, K., H. P. Seyer, F. Hensel: Reflection Spectra of Fluid Sulphur in the Sub- and Supercritical Region 581
– siehe H.-P. Seyer 587
Teliups, W., E. Bauer: Kinetics of the (7 × 7) ↔ (1 × 1) Transition on Si(111) 197
Temps, F., siehe T. Böhland 468
Tenne, R., A. Wold: Photoelectrochemical Etching of n-MoSe₂ 545
Teschner, D. M., R. Schumacher, B. Stritzker: Optical Absorbance and Photoelectrochemical Quantum Efficiency of Titanium Oxide Modified by Ion Implantation and Reductive/Oxidative Annealing 593
Thewissen, D. H. M. W., siehe A. H. A. Tinnemans 383
Thielen, K., siehe K. Natarajan 533
Thomas, H., siehe H.-F. Eicke 872
Thulke, G., siehe P. Gräber 1034
Tielen, M., siehe Th. Bein 395
Tildesley, D. J., siehe Y. P. Yoshi 217
Tinnemans, A. H. A., T. P. M. Koster, D. H. M. W. Thewissen, A. Mackor, J. Schoonman: Photoelectrochemical Properties of Polycrystalline Mg-Doped p-Type Iron(III) Oxide 383
– – A. Mackor, J. Schoonman: Interfacial Phenomena of Polycrystalline Mg-Doped p-Type Iron(III) Oxide Photoelectrodes 390
Tománek, D., siehe H. Dreyssé 245
Träger, F., siehe I. Hussla 240
Tributsch, H., siehe W. K. Hofmann 824
Timmermann, E. O., siehe F. O. Raineri 802
Tringides, M., P. K. Wu, W. Moritz, M. G. Lagally: Ordering Kinetics for O on W(110) 277
Tsang, W., siehe D. A. Robaugh 77
Tse, J. S.: Electronic Structures of the Mono- and Tricarbonyl of Cu and Ag 906
Ueda, W., J. Hiraiwa, N. Yoshida, S. Kishimoto: Catalytic Activity of Colored Sodium Chloride for the Dehydrochlorination of t-Butyl Chloride 353
Uemura, O., T. Sekiya, H. Ishikawa, T. Satow: Electronic and Thermodynamic Properties of the Liquid Tl–AgTe System 71
Ulbricht, W., siehe H. Hoffmann 877
Urushiyama, A., Th. Schönherr, H.-H. Schmidtke: Molecular Structure Determination Inferred from Highly Resolved ⁴A_{2g} ↔ ²E_g, ²T_{1g} Spectra and Ligand Field Calculations of Trigonally Distorted Hexaamminechromate(III) 1188
Vanmackelbergh, D., W. P. Gomes, D. Cardon: Studies on the n-GaAs Photoanode in Aqueous Electrolytes. 3. Recombination Resistance 431
Velasco, I., siehe S. Otin 1179
Vennemann, N., M. D. Lechner, T. Henkel, W. Knoll: Densitometric Characterization of the Main Phase Transition of Dimyristoyl-Phosphatidylcholine between 0.1 and 40 MPa 888
Viehhaus, H., siehe M. Rüsenberg 301
Vojnovic, M. V., siehe A. Damjanovic 1231
Vracar, Lj. M., siehe A. Damjanovic 1231
Wagner, H., R. N. Lichtenthaler: Excess Properties of Liquid Cyclohexane/Hydrocarbon Mixtures. I. Experimental Results of the Excess Enthalpy 65
– – Excess Properties of Liquid Cyclohexane/Hydrocarbon Mixtures. II. Excess Gibbs Energy Determined from Total Vapour Pressure Data 69
– A. Heintz, R. N. Lichtenthaler: Excess Properties of Liquid Cyclohexane/Hydrocarbon Mixtures. III. Application of an Extended Prigogine-Flory-Patterson-Theory 463
Wagner, H. Gg., siehe T. Böhland 468
– siehe W. Möller 854
– siehe W. Hack 1210
Wagner, I., J. Karthäuser, H. Strehlow: On the Decay of the Dichloride Anion Cl₂⁻ in Aqueous Solution 861
Wandelt, K., siehe S. Eder 225
Warnatz, J., siehe B. Rogg 1005
– siehe T. Dreier 1010
Waser, R.: Diffusion of Hydrogen Defects in BaTiO₃ Ceramics and SrTiO₃ Single Crystals 1223
Wasgestan, F., siehe A. Ditze 111
Wedler, G., D. Borgmann, W. Alter, K. Witan: N₂ Adsorbate States on Fe Films between 77 K and 273 K 235
Wehn, R., D. Woermann: Modification of the Electric Double Layer Properties of the Interface

Mica/Aqueous Solution by Adsorption of Polyelectrolytes	121	Wicke, E., siehe H. U. Onken	976	Wold, A., siehe R. Tenne	545
Weiden, N., siehe S. Sharma	725	Wiemhöfer, H.-D., siehe M. Kleinfeld	711	Woldan, M.: Partial Molal Volume of Some Alkali Halides in Water – Acetamide Mixtures	1164
Weidner, J. U., siehe H. Bertagnolli	502	Will, G., siehe R. Becker	833	Wolfrum, J., siehe B. Raffel	997
Weil, K. G., siehe V. W. Benz	201	Willis, R. F.: Critical Fluctuations on Solid Surfaces	190	– siehe T. Dreier	1010
– siehe M. Benje	435	Winter, G.: Anorganische Pigmente: Disperse Festkörper mit technisch verwertbaren optischen und magnetischen Eigenschaften	736	– siehe M. Schneider	1058
Wein, E., W. Müller-Warmuth, R. Schöllhorn: Proton Exchange of Water in Layered Intercalation Compounds	158	Winterlin, J., siehe R. J. Behm	294	Wu, P. K., siehe M. Tringides	277
Weingärtner, H., H. Bertagnolli: The Microscopic Description of Mutual Diffusion and Closely Related Transport Processes in Liquid Mixtures	1167	Witan, K., siehe G. Wedler	235	Wunderlich, I., siehe H. Rehage	1071
Weiss, Ar., siehe I. Dékány	422	Witt, H. T., E. Schlodder, K. Brettel, Ö. Saygin: Reaction Sequences from Light Absorption to the Cleavage of Water in Photosynthesis – Routes, Rates and Intermediates	1015	Yonczawa, Y., D. Möbius, H. Kuhn: Scheibe-Aggregate Monolayers of Cyanine Dyes without Long Alkyl Chains	1183
– siehe I. Dékány	427	Witt, W., E. Bauer: Phase Transitions in Adsorption Layers on bcc(110) Surfaces: S and O on Mo(110)	248	Yoshida, N., siehe W. Ueda	353
Weiss, Al., siehe G. Fecher	1	Woermann, D., siehe R. Wehn	121	Yoshimura, Y., M. Nakahara: Additivity Rule of the Partial Molal Volume. 4. Its Proof Based on the Postulate of Independent Volume Changes for Unit Reactions	58
– siehe G. Fecher	10	– siehe D. Schwahn	339	Zahn, M., siehe T. Dreier	1010
– siehe D. Borchers	718	– siehe P. Schwahn	773	Zellner, R., siehe V. Handwerk	92
– siehe S. Sharma	725			Zimmermann, H. W., siehe H. Bertagnolli	502
– siehe J. Fischer	896			Zumofen, G., siehe A. Blumen	1048
– siehe J. Fischer	1129				
– siehe J. Fischer	1141				
Weller, H., siehe Ch.-H. Fischer	46				

Zeolite Supported Iron Oxide as Catalyst or Catalyst Precursor for Hydrocarbon Conversion Reactions

Thomas Bein*), Mia Tielen, and Peter A. Jacobs**)

Laboratorium voor Oppervlaktechemie, Katholieke Universiteit Leuven, Fakulteit der Landbouwwetenschappen, Kardinaal Mercierlaan 92, B-3030 Leuven (Héverlee), Belgium

Catalysis / Clusters / Iron on Zeolite / Materials Properties / Zeolite Y

When NaY saturated at room temperature with iron pentacarbonyl, is oxidized at room temperature in a very diluted oxygen flow, a zeolite encaged Fe_2O_3 -phase is obtained as shown by Mössbauer spectroscopy, electron microscopy and X-ray diffraction. This catalyst contains 10% by weight of iron and serves as a good precursor of a Fischer-Tropsch (F.T.) catalyst. Unfortunately, the Fe_2O_3 phase is unstable under F.T. conditions, since it is shown that the iron phase migrates out of the zeolite matrix during reaction. — This encaged iron oxide phase can be hydrogen reduced giving finely dispersed and zeolite encaged iron, as is shown by physical and chemical methods.

This system is a stable and active hydrogenolysis catalyst. Its selectivity is influenced by both particle size and support effects.

Introduction

Small iron clusters or iron oxide particles encaged in the pore or channel systems of zeolite supports, catalytically represent attractive systems. Substantial effort has already been reported as far as preparation and characterization are considered. Iron clusters can be generated in zeolites using indirect methods. The classical method, consisting of ion exchanging the zeolite with Fe(II) ions followed by their hydrogen reduction is only applicable to aluminum-rich faujasite-zeolites [1, 2]. Reduction with stronger agents is possible [3, 4], although this easily may result in severe sintering and formation of an extra-zeolitic iron phase. Alternatively, neutral iron complexes, as iron carbonyls, may be adsorbed. Depending on the exact decomposition method this gives rise to the formation of discrete dispersions and particle size distributions [5–13]. Thermal decomposition of sorbed pentacarbonyl inevitably gives a loss of iron [11–13].

A 1% loading of zeolite Y with $\alpha\text{-Fe}_2\text{O}_3$ was obtained using the low temperature adsorption in the solution phase of iron-toluene adducts. Decomposition into $\alpha\text{-Fe}_2\text{O}_3$ seems to occur under influence of residual water. In this way small particle $\alpha\text{-Fe}_2\text{O}_3$ with a diameter of 2.5 ± 0.5 nm is obtained [15]. Recently, the preparation of Fe_2O_3 in the supercages of zeolite NaY with an iron loading of 10% by weight has been reported [16]. Iron pentacarbonyl was adsorbed on dry NaY, followed by exposure of the sample to oxygen at 77 K. In this way, the sorbed carbonyl was gradually oxidized into Fe_2O_3 . Extensive physical characterization indicated this phase to be confined to the intracrystalline void volume of the zeolite. Unfortunately, this system was not stable in Fischer-Tropsch conditions. The reaction selectivity continuously changed till a bulk Hägg carbide phase is formed which exists externally to the zeolite.

In view of what precedes, it was the aim of this work to replace the low temperature oxidation of iron pentacarbonyl by a more realistic operation and to characterize physically

and catalytically the solid thus obtained. An extensive comparison with more classically prepared catalysts is included.

Experimental

The preparation of NaY zeolite containing 10% by weight of iron as adsorbed iron pentacarbonyl was done as described earlier [16]. The sorbed $\text{Fe}(\text{CO})_5$ was transformed into Fe_2O_3 by oxidation at room temperature using a flow of helium, containing 0.1% of oxygen. Reference iron catalysts were prepared by impregnation of silica and γ -alumina with aqueous $\text{Fe}(\text{NO}_3)_3$ solutions so as to obtain a loading of 10% Fe. These supports had a specific surface of 400 and 350 $\text{m}^2 \text{g}^{-1}$, respectively.

Physical characterization of the zeolite-iron associations was done with TEM (transmission electron microscopy), Mössbauer spectroscopy and X-ray diffraction (XRD) spectrometry, in the way described earlier [16].

Catalytic experiments were performed in a continuous flow tubular reactor, the effluent of which was analyzed by on-line gas-chromatography [16]. For the FT experiments the gaseous hourly space velocity was 1000 at the reactor entrance. The reactant pressure was 2.0 M Pa and the CO/H_2 molar ratio 0.73. The n-decane hydrogenolysis was done at atmospheric pressure, using a weight hourly space velocity of 1.2 and a hydrogen/decane molar ratio of 10.

Results

Preparation and Physical Characterization of FeO_x on Zeolite NaY

Dry zeolite NaY was equilibrated in the dark at 295 K with iron pentacarbonyl and subsequently degassed purging the sample with dry helium. The sample contained on the average three residual $\text{Fe}(\text{CO})_5$ molecules per supercage, which corresponds to 10% by weight of iron. To the purge gas was then added 0.1% of oxygen, in order to oxidize the adsorbed $\text{Fe}(\text{CO})_5$ gradually and transform it into adsorbed Fe_2O_3 . No overheating in the catalyst bed could be detected during the oxidation reaction. This sample will be denoted as NaY/ FeO_x^* to discriminate it from the NaY/ FeO_x sample described earlier [16], which was loaded with carbonyl in a similar way but overheating during oxidation was avoided by cooling the sample down to 77 K, exposing it to oxygen at this temperature and allowing it to warm up to room temperature.

The physical characterization of this sample was almost identical to the one described earlier, which was prepared much more cautiously but using rather unrealistic conditions [16]. The present sample shows a six-line Mössbauer pattern at 1.8 K, with a hyperfine field of 43 T and an isomer shift of 0.3 mm s^{-1} (Fig. 1). At room

*) Present address: Du Pont de Nemours, Experimental Station, Wilmington, Delaware 19898, USA.

***) Author for all correspondence.

temperature, this six-line spectrum relaxes to give a symmetrical doublet with a quadrupole splitting of $V_{zz} = 1.0 \text{ mm s}^{-1}$.

This Mössbauer behaviour also indicates that NaY/FeO_x^* and NaY/FeO_x are identical materials. TEM and XRD confirm this, since at magnifications of 300 000 times, the supported iron system in both cases does not display any particles. In the XRD pattern, also no lines not ascribable to the NaY-zeolite could be detected.

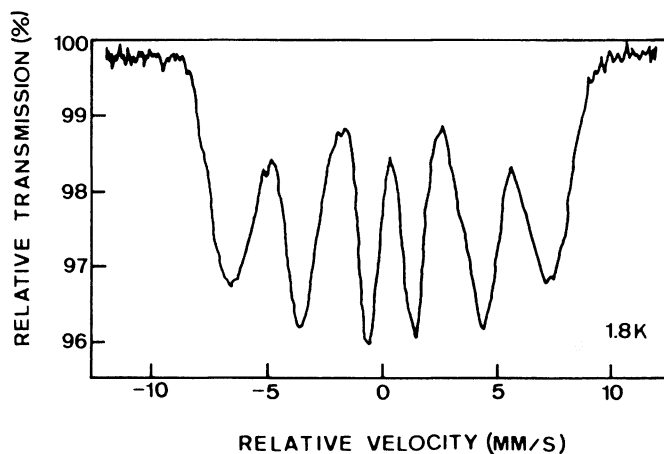


Fig. 1

Mössbauer spectrum of sample NaY/FeO_x^* measured at 1.8 K. The lines are drawn by connecting the measured data points

Table 1
Comparison of NaY/FeO_x^* and NaY/FeO_x ¹⁾ zeolites as Fischer-Tropsch catalysts at a temperature of 555 K

Catalyst	Time-on-stream (hours)	CO conversion (%)	Growth factor for C_3-C_8	Growth factor for C_8-C_{16}
NaY/FeO_x	0.5	36.8	0.644	—
NaY/FeO_x^*	0.6	38.0	0.649	—
NaY/FeO_x	120.0	25.8	0.657	0.875
NaY/FeO_x^*	127.0	26.3	0.651	0.861

¹⁾ Data on this catalyst are from Ref. [16].

Behaviour of NaY/FeO_x^* as a Fischer-Tropsch (F.T.) Catalyst

The F.T. behaviour of NaY/FeO_x has been investigated in detail [16]. At increasing times-on-stream, this sample slightly deactivates and the hydrocarbon growth factor steadily increases for longer reaction times. This means that heavier hydrocarbons desorb from the catalyst at longer reaction times. In Table 1, some pertinent data are given, which compare the behaviour of catalyst NaY/FeO_x to that of NaY/FeO_x^* . Within experimental error, both materials behave as identical F.T. catalysts. When two different growth factors are mentioned in Table 1, this indicates that two sets of active F.T. sites are present. This is true at steady state on both catalysts. The physical characterization of the equilibrium NaY/FeO_x catalyst [16], indicates that during the F.T. reaction part of the active phase migrates out of the zeolite and is transformed into a Fe_xC phase.

Since this sintering is possibly caused by the steam atmosphere present during a F.T. reaction, the behaviour of sample NaY/FeO_x^* in less demanding conditions was also investigated.

Characterization of Reduced NaY/FeO_x^*

NaY/FeO_x^* is a suitable precursor for zeolite supported iron since the Fe_2O_3 -phase is confined to the cages of the zeolite. A NaY/Fe

catalyst was generated during reduction of this precursor either at 573 or 873 K. Reference catalysts carry equal amounts of iron on the classical supports γ -alumina and silica. The latter were prepared via an impregnation with $\text{Fe}(\text{NO}_3)_3$, drying, calcination at 823 K and subsequent reduction at 573 and 873 K, respectively.

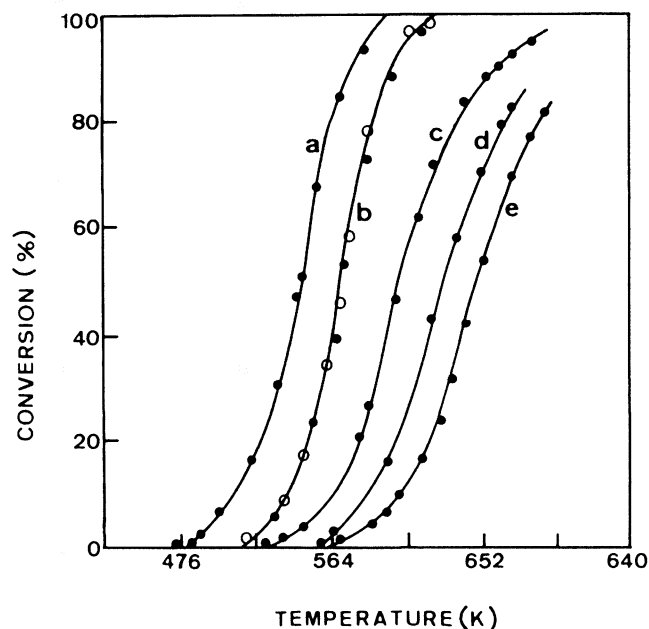


Fig. 2

n-Decane hydrogenolysis over 10% Fe on support catalysts: a) silica-873; b) silica-573 (open points); b) NaY -873 (full points); c) NaY -573; d) alumina-873 and e) alumina-573.

The characterization of reduced Fe_2O_3 , on NaY, alumina and silica by CO chemisorption, Mössbauer spectroscopy and XRD spectrometry is given in Table 2. The Mössbauer data indicate that in every case the Fe_2O_3 supported phase is reduced completely. At the two reduction temperatures used, all iron is kept inside the cages of the zeolite as shown by X-ray diffraction. Also on alumina, the dimensions of the iron particles remain in both cases below the detection limit of this technique, while on silica definitely larger iron particles are formed in comparable conditions. These trends are confirmed by the CO-chemisorption data. Indeed, on alumina and NaY a similar degree of metal dispersion is achieved, while on silica, the metal dispersion is lower. For all catalysts, an increased degree of sintering is found after the high temperature reduction.

Hydrogenolysis of n-Decane over Supported Iron Catalysts

Catalytic data for the hydrogenolysis of n-decane over the iron catalysts discussed above are presented in Table 3 and 4 and Fig. 2. While an apparent activation energy is found in the small range from 34 to 41 kJ mol^{-1} for all catalysts, a strong effect of the catalyst on the reaction rate can be observed (Table 3). With all three supports a higher reaction rate is noted when iron oxide is reduced at higher temperature. This treatment results in a lower iron dispersion. Iron dispersion however, is not the only rate determining parameter. At approximately 70% iron dispersion (Table 3), the hydrogenolysis rate is support dependent and decreases as follows:

silica > NaY > alumina .

Further insight into the structure-sensitivity of the decane hydrogenolysis reaction is obtained if the detailed product selectivities are compared (Table 4).

Table 2
Characterization of reduced Fe₂O₃ on different supports

Support	Reduction temperature (K)	CO chemisorption CO/Fe × 100	Mössbauer hyperfine splitting (T)	Isomershift relative to bulk Fe (mm s ⁻¹)	Intensity of Fe(111) reflection
NaY	573	90	33.1	0.0	— ¹⁾
	873	68	33.1	0.0	—
alumina	573	90	33.1	0.0	—
	873	72	33.1	0.0	—
silica	573	75	33.1	0.0	+ ²⁾
	873	50	33.0	0.0	+ + ³⁾

¹⁾ absent; ²⁾ visible; ³⁾ fairly, intense.

Table 3
Reaction rates for n-decane hydrogenolysis on supported iron catalysts¹⁾

Catalyst	Iron dispersion ²⁾ (%)	Reduction temperature (K)	Reaction rate (r) at 540 K (mmol g ⁻¹ s ⁻¹ 10 ⁶)	Apparent activation energy (E _a) (kJ mol ⁻¹)
Fe/NaY-573	90	573	1830	37.50
Fe/NaY-873	68	873	2650	34.50
Fe/alumina-573	90	573	324	41.08
Fe/alumina-873	72	873	1320	—
Fe/silica-573	68	573	4550	39.70
Fe/silica-873	50	873	6830	—

¹⁾ Containing each 10% by weight of iron.

²⁾ From Table 2.

Table 4
Distribution of the hydrogenolysis products from n-decane over 10% Fe on support catalysts

Catalyst	Fe dispersion ¹⁾ (%)	Conversion (%)	Product distribution per carbon number (mol per 100 mol converted)								
			C ₁	C ₂	C ₃	C ₄	C ₅	C ₆	C ₇	C ₈	C ₉
alumina-573	90	10	524	16	10	9	8	8	8	10	9
NaY-573	90	10	399	16	14	13	10	10	10	10	15
NaY-873	68	10	213	26	8	8	6	6	5	21	44
silica-573	75	10	113	33	17	6	6	6	3	5	67
alumina-873	72	60	657	17	8	7	6	5	5	5	5
NaY-873	68	60	582	21	12	9	8	8	7	6	7
silica-873	50	60	135	15	12	10	10	10	9	10	11

¹⁾ From Table 2.

The catalytic stability of the iron on NaY catalyst is remarkably good. The presented trends derived from kinetic and product distribution data obtained after 2 hours on-stream, remain virtually unchanged after 24 hours on stream.

Discussion

The assignment of the Mössbauer spectra of NaY/FeO_x to α-Cl or γ-Fe₂O₃ associated with the zeolite has been discussed earlier [16]. In this work a survey of literature Mössbauer parameters of supported and bulk α and γ-Fe₂O₃ and of Fe₂O₄ is made and compared to those of the NaY/FeO_x sample. It follows that the NaY/FeO_x and consequently the

NaY/FeO_x* sample consists of a α-Cl or γ-Fe₂O₃ phase intimately associated with the zeolite. The other physical measurements (XRD and TEM) confirm this and suggest that the iron oxide is dispersed in the intracrystalline void volume of the Y zeolite.

The F.T. behaviour of both materials also is identical, confirming the conclusions drawn from the physical characterization measurements. Characterization of an equilibrium NaY/FeO_x catalyst in a F.T. experiment has shown that during the transient behaviour a significant part of the iron sinters out of the zeolite and is transformed into a Fe_xC phase. The similarity in catalytic behaviour between NaY/

FeO_x and NaY/FeO_x^* , suggests that the same transformations occur on the NaY/FeO_x^* sample, prepared according to the presently presented method. The presence of two discrete hydrocarbon chain growth factors is in line with the presence of two sets of active sites, a bulk carbide phase located externally to the zeolite crystals and residual iron still present in the zeolite cages. The present data do not allow to make any conclusions as to the nature of the latter phase: oxidic, metallic or carbidic.

The absence of any deactivation during the hydrogenolysis reaction clearly indicates that sintering of finely dispersed iron oxide during the F.T. reaction is not caused by the presence of a hydrocarbon atmosphere, but rather by the high partial pressure of water generated during the F.T. reaction. On the other hand, it seems that hydrogen reduction of Y zeolite supported Fe_2O_3 , prepared by mild oxidation of adsorbed pentacarbonyl, constitutes a gentle method for the preparation of finely dispersed iron in the cages of zeolite Y. This is not possible when Fe(III)-exchanged Y zeolite is used as starting material [1, 2].

The decane hydrogenolysis reaction rate on zeolites, just like on other supports is shown to be dispersion-dependent. The higher the iron dispersion, the lower is the hydrogenolysis rate. This behaviour is expected for a structure-sensitive reaction [18]. The data also indicate that at comparable iron dispersion the hydrogenolysis rate is support dependent. The observed decrease in hydrogenolysis rate according to the sequence:

silica > NaY > alumina

has been found earlier with other materials (Pt, Pd) and for other reactions (e.g. benzene hydrogenation) [17]. It corresponds to an increasing acidity or electron withdrawing capability of the respective supports. The dependence of catalyst activity upon the degree of dispersion and the nature of the support remains unchanged over the whole conversion range of the feed molecule, as can be derived from Fig. 2. The unchanged activation energy suggests that similar reaction paths exist on the iron surface of the catalysts, whereas the strong dependence of activity on metal dispersion is the result of an increased number of active sites available on the iron phase as its dispersion decreases. This classifies the n-decane hydrogenolysis as a structure-sensitive reaction, in agreement with the earlier findings of Sinfelt [18].

As far as the reaction mechanism is concerned this indicates that preferentially C_1 species are chopped from the longer hydrocarbon chain (Table 4). Although this seems to be a property of iron as catalyst, it can be amplified by increasing the dispersion of the metal or at a given dispersion by increasing the electron accepting properties of the support. These influences fit nicely in the Sinfelt picture [17] for ethane hydrogenolysis. The intermediates in this reaction are highly unsaturated hydrocarbon residues multiply bonded to surface metal atoms. The reaction is therefore dependent on the presence of specific geometric arrangements of surface atoms or of their electronic properties. The existence of both phenomena is evidenced by alloy dilution experiments and correlations with the percentage d-character of the catalytic elements respectively [18].

The two parameters determining the activity are found to influence the product distribution as well. It is obvious that with higher dispersion of iron an increased selectivity for methane compared to all other products is observed. At both conversion levels, the support effect at identical dispersion on the methane selectivity is clearly present. Indeed, the methane yield increases as follows:

at 10% conversion: silica-573 < NaY-873

at 60% conversion: NaY-873 < alumina-873 .

The molar distribution among C_5 is still asymmetrical even when abstraction is made from C_1 and C_9 . This asymmetry is more pronounced at the high conversions.

It is well established that the nature of the catalytic element determines also the product distribution in the hydrogenolysis reaction. Ni attacks selectively the ends of alkane chains, whereas Pt is the other extreme since it breaks statistically all C—C bonds [19]. The iron catalysts represent examples of the former type of cleavage, with preference for attack at the end of the hydrocarbon. This preference is definitely less pronounced on iron compared to nickel, but it seems that degree of metal dispersion and support influence can modify this behaviour.

Financial support for this research comes from the Belgian Government (Concerted Action on Catalysis). P. A. J. acknowledges NFWO-FNRS for a research position.

References

- [1] Y. Y. Huang and J. R. Anderson, *J. Catal.* **40**, 143 (1975).
- [2] R. L. Garten, W. N. Delgass, and M. Boudart, *J. Catal.* **18**, 19 (1970).
- [3] F. Schmidt, W. Gunsser, and J. Adolph, *A. C. S. Symp. Ser.* **40**, 291 (1977).
- [4] L. B. Lee, *J. Catal.* **68**, 27 (1981).
- [5] D. Ballivet-Tkatchenko, G. Coudurier, H. Mozzanega, and I. Tkatchenko, *Fund. Res. Homog. Catal.*, p. 257, ed. Tsutsui, New York 1979.
- [6] D. Ballivet-Tkatchenko and G. Coudurier, *Inorg. Chem.* **18**, 558 (1974).
- [7] D. Ballivet-Tkatchenko, N. D. Chau, H. Mozzanega, M. C. Roux, and I. Tkatchenko, *A. C. S. Symp. Ser.* **152**, 187 (1981).
- [8] D. Ballivet-Tkatchenko, G. Coudurier, and N. D. Chau, *Stud. Surf. Sci. Catal.*, Elsevier **19**, 123 (1982).
- [9] L. F. Nazar, G. A. Ozin, F. Hugues, J. Godber, and D. Rancourt, *J. Molec. Catal.* **21**, 313 (1983).
- [10] J. B. Nagy, M. van Eenoo, and E. G. Derouane, *J. Catal.* **58**, 230 (1979).
- [11] F. Schmidt, Th. Bein, U. Ohberich, and P. A. Jacobs, *Sixth Int. Zeolite Conf.*, p. 151, eds. D. Olson and A. Bisio, Butterworth 1984.
- [12] Th. Bein, F. Schmidt, and P. A. Jacobs, *Int. Symp. Zeolites, Portrose 1984*, in press.
- [13] A. X. Trautwein, E. Bill, R. Bläs, G. Doppler, F. Seel, B. Wolf, R. Klein, and U. Gonser, *Surf. Sci.* **156**, 140 (1985).
- [14] D. G. Rancourt, S. R. Julian, and J. M. Daniels, *J. Magnet. Magn. Mater.* **49**, 305 (1985).
- [15] L. F. Nazar, G. A. Ozin, F. Hugues, J. Godber, and D. Rancourt, *J. Mol. Catal.* **21**, 313 (1983).
- [16] Th. Bein, G. Schmiester, and P. A. Jacobs, *J. Phys. Chem.* **1986**, in press.
- [17] F. Figueras, R. Gomez, and M. Primet, *Adv. Chem. Ser.* **121**, 480 (1973).
- [18] J. H. Sinfelt, *Catal. Rev. Sci. Eng.* **9**, 147 (1974).
- [19] J. E. Germain, "Catalytic Conversion of Hydrocarbons", p. 119, Academic Press 1969.

(Eingegangen am 16. Dezember 1985,
endgültige Fassung am 20. Januar 1986)

E 6170